



## MODELING OF NONDUCTILE R/C COLUMNS SUBJECTED TO EARTHQUAKE LOADING

J.A. PINCHEIRA and F.S. DOTIWALA

Department of Civil and Environmental Engineering, University of Wisconsin-Madison,  
Madison, WI 53706, U.S.A.

### ABSTRACT

Nonlinear analysis of older reinforced concrete buildings under seismic loading requires modeling of members with nonductile behavior. This paper presents modifications of an existing model to simulate the shear failure of reinforced concrete columns. Main characteristics of the model include shear strength decay with increasing displacement amplitude and with loading cycles. Predicted response is compared with experimental data obtained from tests of columns with substandard details. The results show good agreement between predicted and measured response.

### KEYWORDS

Seismic rehabilitation; seismic retrofit; reinforced concrete; shear strength; nonlinear models.

### INTRODUCTION

Reinforced concrete frames designed according to older code provisions have often performed inadequately during past earthquakes. A poor lateral load resisting system (often with strong beams and weak columns) combined with inadequate detailing of the reinforcement in frame members are the main reasons for the severe damage and partial or total collapse observed after strong shaking. In columns, poorly confined, short lap splices in potential hinging regions (usually right above the floor level) can result in reduced flexural capacity and limited rotational ductility. Also, wide spacing of the transverse reinforcement can often lead to column shear failure with a rapid strength and stiffness degradation under cyclic loading. In recent years, the behavior of building columns containing substandard reinforcing details has been investigated experimentally (Aboutaha et al., 1994, Moehle et al., 1995). These and other studies show that, depending on the reinforcement details, a column designed according to past standards may develop yielding of the longitudinal reinforcement and reach modest levels of displacement ductility before reaching its shear capacity. In other cases, columns may exhibit failure of splices prior to or concurrently with shear failure, or may reach their shear capacity without flexural yielding or splice failure. In general, the behavior of these columns is characterized by limited deformation capacity, and by strength and stiffness degradation with increasing displacement amplitude and with loading cycles.

In this paper, an analytical model developed to emulate the seismic response of columns with substandard reinforcing details is presented. The focus of the paper is on the shear behavior of such columns, although the model can accommodate nonlinear behavior in flexure (yielding or splice failure) and shear.

## SHEAR STRENGTH OF REINFORCED CONCRETE COLUMNS

Many existing design models are based on the idea that shear strength can be estimated as the sum of the shear strength of the concrete,  $V_c$ , and the strength provided by the transverse reinforcement,  $V_s$ . Under earthquake loading, the shear strength of a reinforced concrete column will degrade. Although the sources of strength degradation include several factors, the reduction in overall shear strength is usually accounted for by reducing the contribution of the concrete to shear strength,  $V_c$ . Close evaluation of existing data combined with the results of recent tests of both bridge and building columns, have reinforced the notion that shear strength decreases with increasing amplitude of deformation or level of displacement ductility. Some design models assume that the initial shear strength can be sustained only for small displacement ductility levels (Aschheim et al., 1993, ATC, 1983, Priestley et al., 1992) and suggest a linear reduction of the shear capacity as the displacement ductility increases. At large displacement ductility levels, the shear strength of the member can be represented by a residual shear strength,  $V_r$ . This residual strength is usually assumed to be provided by the transverse reinforcement alone without any contribution from the concrete. The shear model presented in the following was largely based on these observations and was developed with the purpose of employing the model for the seismic evaluation of existing, nonductile reinforced concrete frames.

## ANALYTICAL MODEL

### *Description of the Element*

The element presented here is a variation of the one-component model (Giberson, 1969). In this model, all inelastic deformations are assumed to be concentrated in zero-length plastic hinges at the element ends. Structural members are idealized by a linear elastic sub-element with nonlinear springs (zero-length plastic hinges) at the element ends. The original element consisted of one nonlinear spring at each end that accounted for flexural yielding and strain hardening. This model followed hysteresis rules proposed by Takeda and Sozen (1970) and was incorporated into the DRAIN-2D computer program (Kannan et al., 1972). In a more recent study, the element was modified to model the behavior of members with a splice or anchorage failure by introducing flexural strength degradation with increasing rotational amplitude (Pincheira et al., 1992).

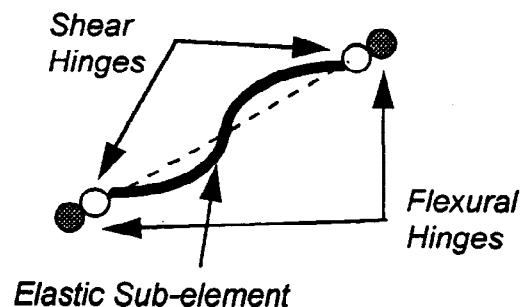


**Figure 1** One component model with nonlinear springs.

In this study, the element was further modified to include strength and stiffness degradation due to shear failure. The model for shear follows the concepts proposed by Chen and Powell (1982) and is similar to that presented by Ricles et al. (1991) with some modifications. Nonlinear behavior in shear is accomplished by adding a zero-length shear hinge or nonlinear shear spring connected to the elastic sub-element at the ends as shown in Fig. 1. Nonlinear behavior in flexure is assumed to be independent of that in shear. However, equilibrium between member bending moments and shear force is maintained at all times. The addition of the shear hinge to the existing element permits nonlinear flexural behavior (yielding or splice failure) to occur concurrently with nonlinear behavior in shear.

## Hysteretic Laws

Hysteresis laws for the element with flexural hinges as modified to emulate the failure of splices have been presented elsewhere and will not be discussed here (Pincheira et al., 1992). Fig. 2 shows the shear and displacement envelope (primary curve) for the element with shear hinges alone. Behavior of the member is assumed to be linear elastic until the onset of shear cracking,  $V_{cr}$ . In this range, shear hinges are assumed to be rigid and thus the member's stiffness is that of the elastic sub-element alone. Following shear cracking, the member follows a reduced shear stiffness (shear hinges are no longer rigid) but continues to carry additional loading until the maximum shear strength,  $V_{max}$ , is reached. Upon further increase in lateral displacement, the member shear strength decreases with increasing displacement amplitude until the member reaches its residual shear capacity,  $V_r$ . Such behavior is assumed to be the same in both directions of lateral displacement.

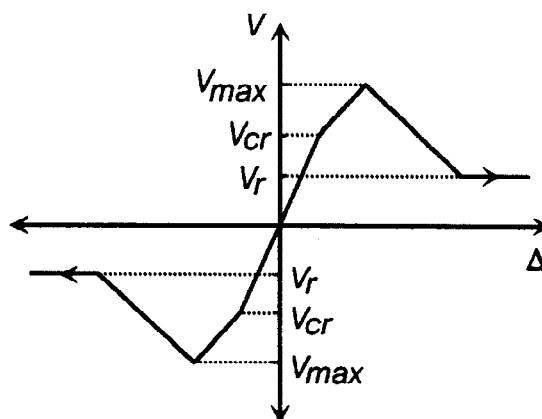
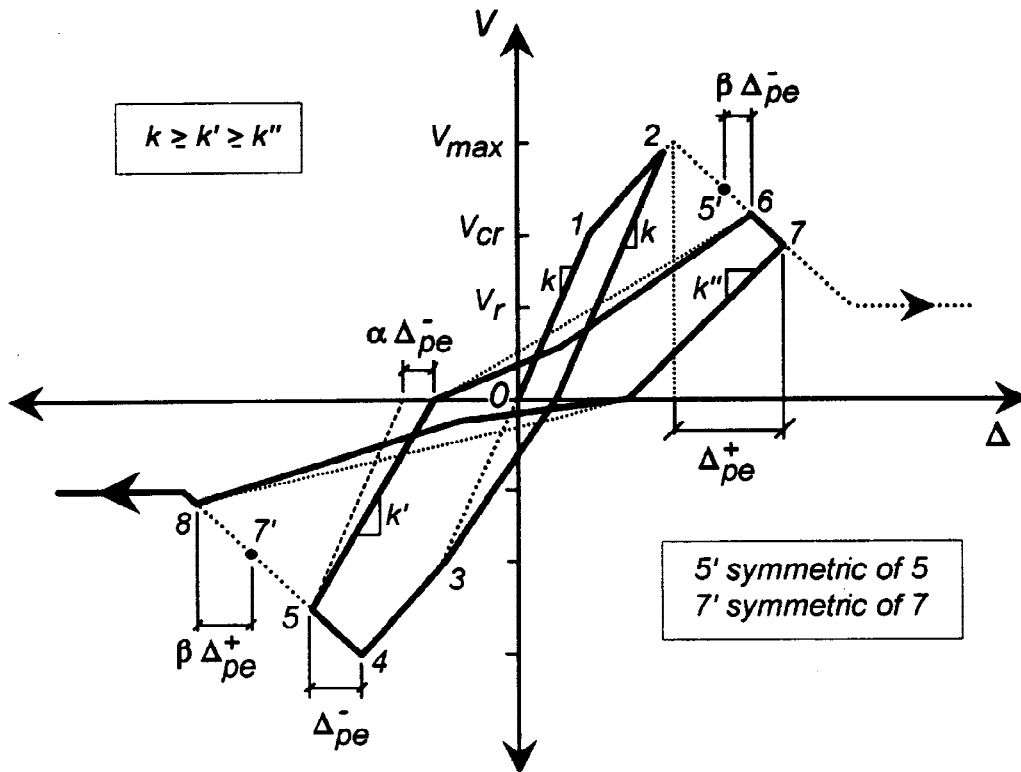


Figure 2 Shear and displacement envelope.

Fig. 3 illustrates hysteretic behavior for loading cycles corresponding to events on the primary curve. In this figure, segments 0-1 and 1-2 illustrate the behavior of the member when loaded above the shear cracking strength,  $V_{cr}$ , but below the maximum shear strength,  $V_{max}$ . If the member is unloaded at this stage (point 2 on the primary curve), there is no stiffness degradation upon unloading. Loading in the opposite direction of displacement is then directed toward the shear cracking strength of the member,  $V_{cr}$ , as shown in the figure. Further loading in the same direction of displacement will follow a reduced shear stiffness until the maximum shear strength,  $V_{max}$ , is reached (segments 1-2 and 3-4 are assumed to have the same slope). If the imposed displacement exceeds that corresponding to the maximum shear strength,  $V_{max}$ , the shear strength decreases with increasing displacement amplitude as shown in Fig. 3 (segment 4 - 5). Upon reversal of the imposed displacement at this stage (point 5 on the primary curve), the member unloads with a reduced stiffness. The unloading stiffness is reduced by an amount that depends on the maximum plastic deformation attained in the current inelastic excursion ( $\Delta_{pe}^-$  in Fig. 3) and a controlling parameter  $\alpha$ . If the member is then loaded in the opposite direction, the reloading stiffness is calculated by defining point 6 on the primary curve. This point has a plastic deformation equal to or larger than that attained during the inelastic excursion in the opposite direction (plastic deformation corresponding to point 5). Such a law was introduced to account for strength degradation upon load reversals and is controlled by a parameter  $\beta$  as shown in Fig. 3. Pinching of the hysteresis loops can be included in the model. The amount of pinching depends on the reloading stiffness and a controlling parameter  $\gamma$ . The sequence of events just described is similar for subsequent cycles as shown by segments 6 - 7 - 8 in Fig. 3.

Hysteretic laws for internal cycles (i.e., cycles with displacement amplitudes smaller than those corresponding to events on the envelope curve) are shown in Fig. 4. Behavior of the model during the first loading cycle is the same as that described above for loading cycles corresponding to events on the primary curve (segments 0 - 1 - 2 - 3 - 4 - 5). If, however, the imposed displacement amplitude upon reloading (point 6 in Fig. 4) is smaller than that associated with the maximum attainable shear strength in the current cycle (point A in Fig. 4), there is no stiffness degradation upon unloading (segment 6 - 7). Reloading in the opposite direction of displacement is directed toward point B on the primary curve. This point has a plastic deformation equal to or greater than that of point A (the maximum attainable shear strength defined by the most recent inelastic excursion in the opposite direction). In this manner, it is



**Figure 3** Hysteretic laws for cycles corresponding to events on the primary curve.

possible to account for shear strength degradation for loading cycles that do not result in events on the primary curve. The amount of strength degradation depends on the maximum plastic deformation attained in the most recent inelastic excursion in the opposite direction,  $\Delta^+_{pe}$ , and is controlled by a parameter  $\eta$ , as shown in Fig. 4. Experimental evidence shows that the rate of strength degradation within cycles of equal displacement level diminishes with the number of loading cycles. Such an effect is accounted for in the model by reducing the value of the parameter  $\eta$  in subsequent internal cycles (segments 8-9-10). Pinching of the hysteresis loops is considered in a manner similar to that mentioned above for cycles corresponding to events on the primary curve. For internal cycles with displacement amplitudes smaller than those corresponding to the maximum shear capacity,  $V_{max}$ , it is assumed that there is no strength degradation, i.e., the parameter  $\eta$  is zero.

The shear and displacement envelope can be defined from a combination of existing predictive equations and experimental observations. The maximum shear strength,  $V_{max}$ , can be estimated as the initial strength of the column, while the residual strength,  $V_r$ , can be estimated as the strength provided by the transverse reinforcement alone using the predictive equations available in the literature. The shear cracking strength,  $V_{cr}$ , may be more difficult to predict but can be reasonably estimated as the shear strength provided by the concrete  $V_c$ . The rest of the parameters required by the model (stiffness of the member at different stages, rate of strength and stiffness degradation and amount of pinching) can only be determined from experimental data at this time.

## COMPARISON OF ANALYTICAL MODEL AND EXPERIMENTAL RESULTS

In the following, the model described above is compared with the experimental results of two reinforced concrete columns. These columns were designed according to past design standards and exhibited a shear dominated behavior with essentially no flexural ductility. The analytical results presented below include only nonlinear behavior in shear, i.e., the flexural hinge was assumed to remain rigid.

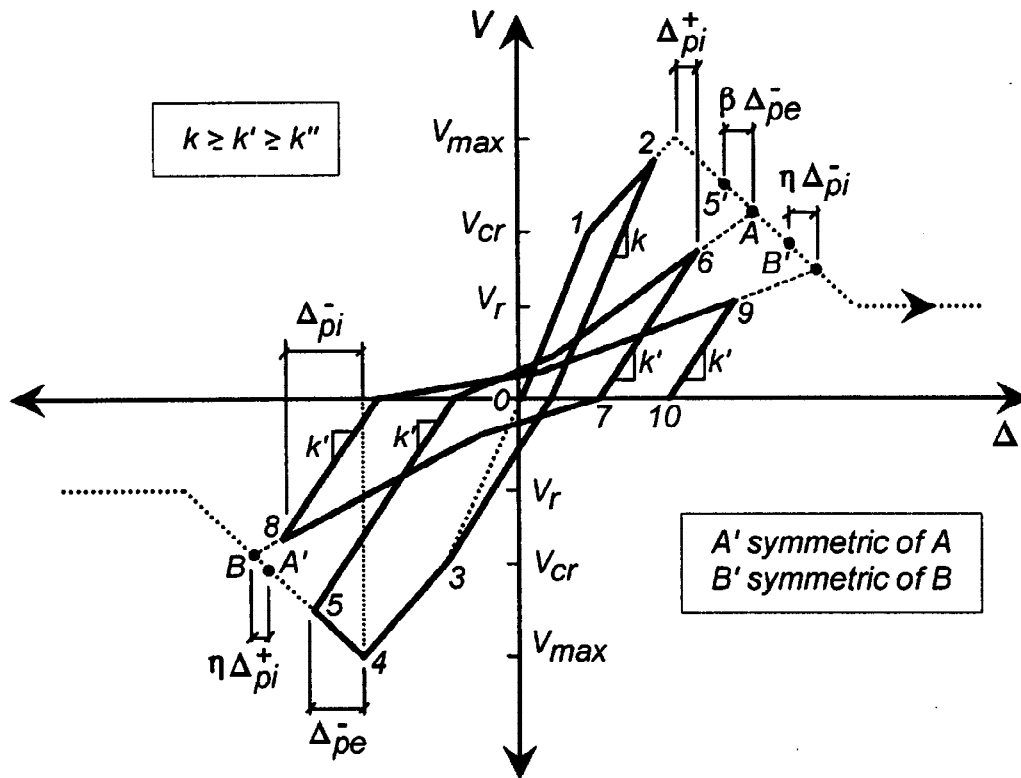


Figure 4 Hysteretic laws for internal cycles.

The first column selected for comparison is an 18 inch square column tested in double curvature under reversed cyclic loading (Moehle et al., 1995). Column reinforcement consisted of eight #10 reinforcing bars with #3 perimeter hoops spaced at 18 in. All reinforcement was Grade 40. No splices were provided. An axial load of  $0.1 A_g f'_c$  was maintained during the tests. Fig. 5 shows the experimental and analytical results for this column. In this figure, the analytical response was obtained using the measured shear strengths for the column. Overall, the results show good agreement between the measured and the predicted response. For small amplitude cycles, the test results show some nonlinear and hysteretic behavior, probably due to flexural cracking. Such behavior, however, is not predicted by the model as nonlinear behavior in shear will only begin after the shear cracking strength is reached (flexural hinges were assumed to remain rigid in this example). Also, for the specified parameters the model appears to overestimate the amount of pinching within the first cycle after reaching the maximum shear strength.

The second column is an 18 by 36 inch rectangular column. The specimen was of a cantilever type and was loaded for strong axis bending (Aboutaha et al., 1994). The longitudinal reinforcement consisted of sixteen #8 Grade 60 reinforcing bars. Transverse reinforcement in the direction of the applied shear consisted of #3 Grade 40 perimeter hoops spaced at 16 in. No axial load was applied to the column during the test. The measured and predicted response are shown in Fig. 7. Overall, good agreement exists between the experimental and analytical results.

The results presented here correspond to columns where no significant flexural yielding occurred before reaching the maximum shear capacity. As mentioned earlier, it is also possible for columns to develop flexural yielding and exhibit some level of displacement ductility before failing in shear. In such cases the shear strength will be reduced as the displacement ductility increases. While the present element can accommodate concurrent nonlinear behavior in flexure and shear, it cannot account for reductions in shear strength with increasing displacement ductility. Modifications to the element to include such effects are underway.

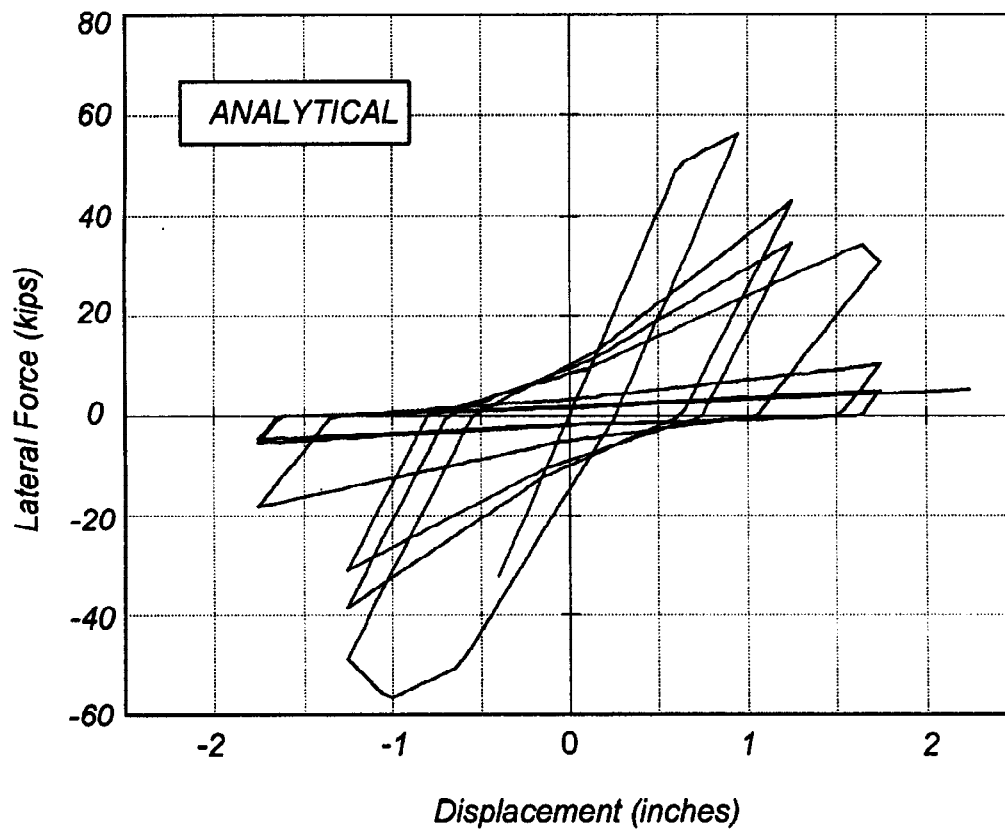
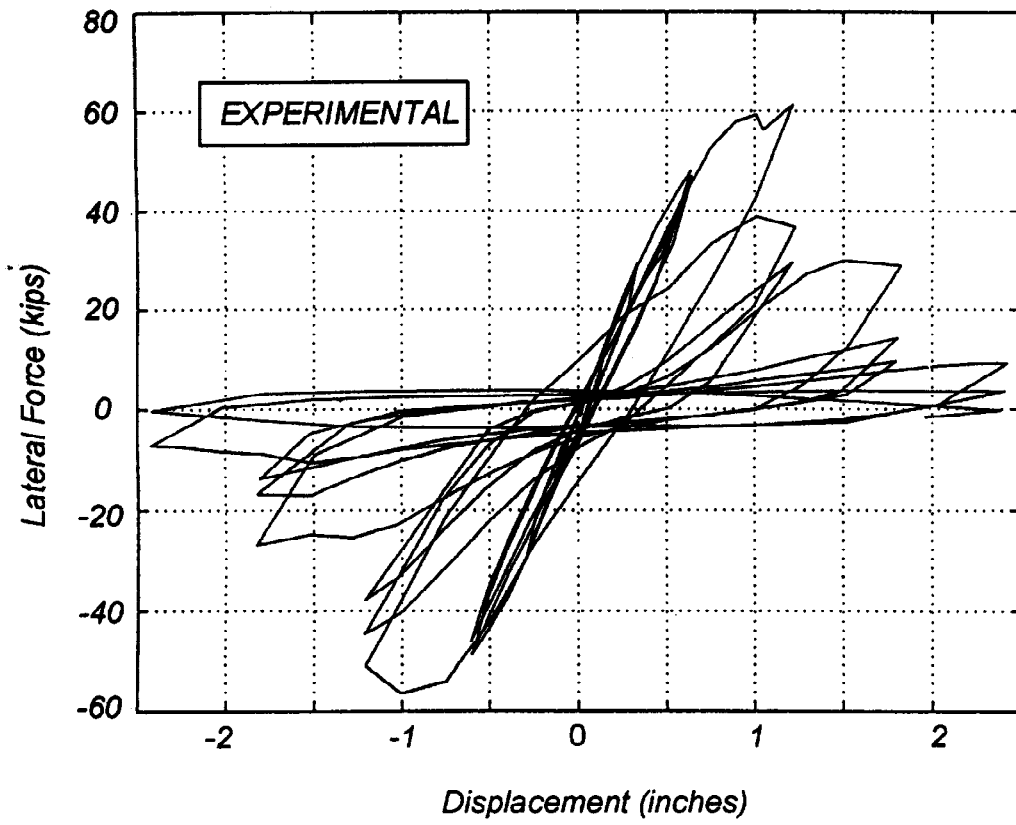


Figure 5 Comparison of analytical and experimental results, square column.

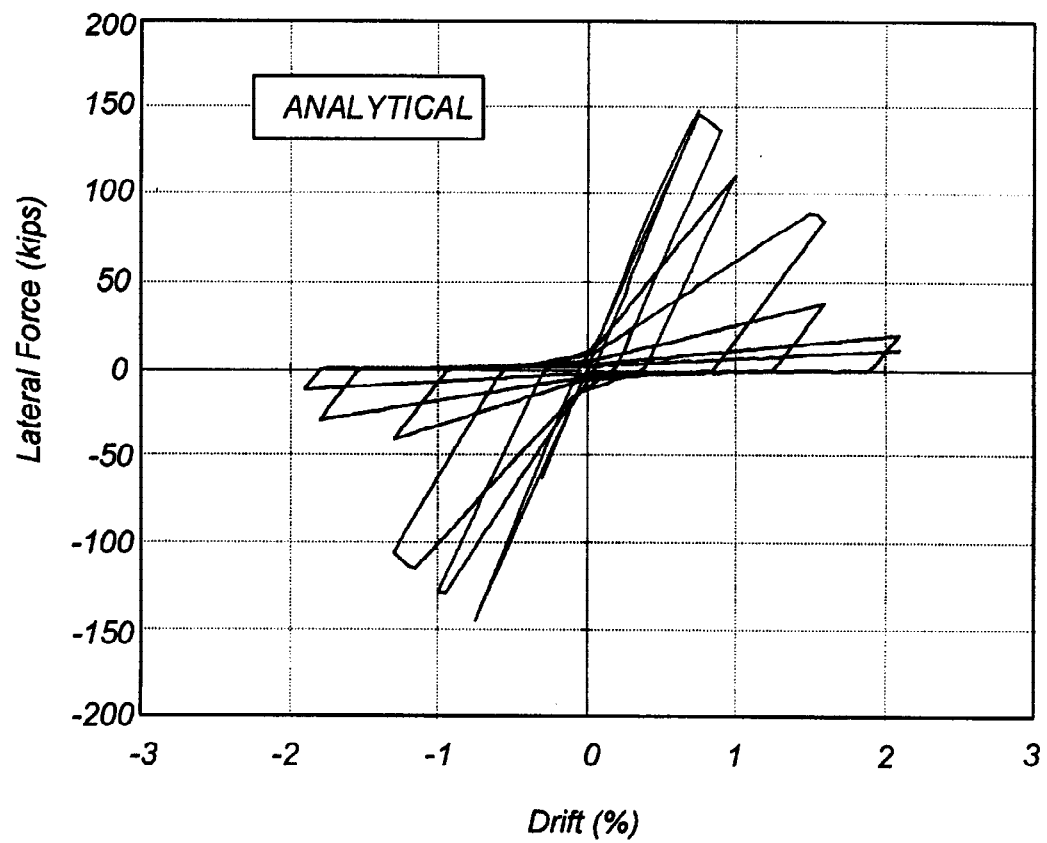
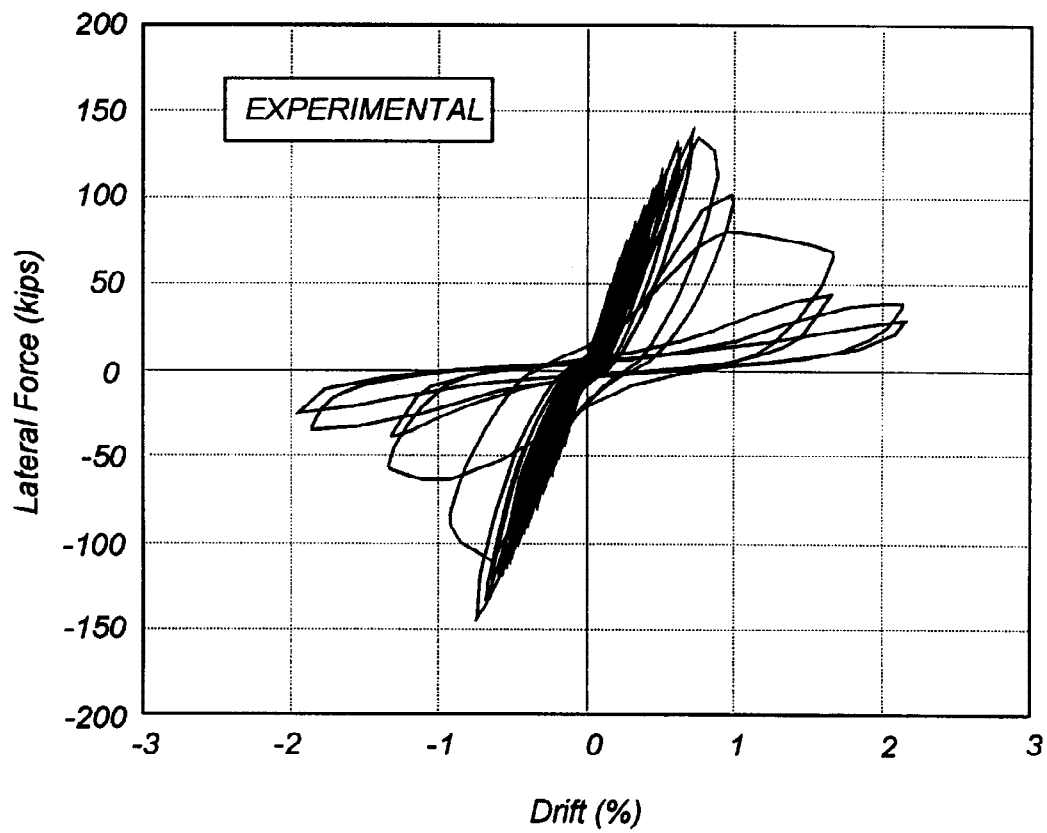


Figure 6 Comparison of analytical and experimental results, rectangular column.

## CONCLUSIONS

An analytical model to simulate the nonlinear response in flexure and shear of non-ductile reinforced concrete columns is presented. Main characteristics of the model presented herein include shear strength and stiffness degradation with cycles and with increasing displacement amplitude. Predicted and measured response are compared for two columns with shear dominated behavior. The results show good agreement between observed and predicted behavior. The reduction in the initial shear strength with increasing displacement ductility observed for yielding columns cannot be captured by the present model; however, modifications to include such effects are in progress.

## REFERENCES

- Aboutaha, R.S., Engelhardt, M.D., Jirsa, J.O. and Kreger, M.E. (1994). Seismic shear strengthening of R/C columns using rectangular steel jackets. *Proceedings of the Fifth U.S. National Conference on Earthquake Engineering, Volume III*, pp. 799-808.
- Aschheim, M., Moehle, J.P. and Werner, S.D. (1993) Deformability of concrete columns. *Technical Report prepared for California Department of Transportation, Division of Structures, Sacramento, California.*
- Applied Technology Council, ATC. (1983) Seismic retrofitting guidelines for highway bridges. *Report ATC-6-2, Palo Alto, California.*
- Chen, P.F. and Powell, G.H. (1982) Generalized plastic hinge concepts for 3D beam-column elements. *Report No. UCB/EERC-82/20, Earthquake Engineering Research Center, University of California at Berkeley, Berkeley, California.* 267 pp.
- Giberson, M.F. (1969). Two nonlinear beams with definition of ductility. *Journal of the Structural Division, ASCE, Volume 95, No. ST2*, pp. 137-157.
- Moehle, J. P and Lynn, A.C. (1995). Private communication. *University of California at Berkeley, Berkeley, California.*
- Kannan, A.E., and Powell, G.H. (1973) DRAIN-2D: A general purpose program for dynamic analysis of inelastic plane structures. *Report No. EERC 73-6, University of California, Berkeley.*
- Pincheira, J.A., and Jirsa, J.O. (1992) Seismic strengthening of reinforced concrete frames using post-tensioned bracing systems. *PMFSEL Report No. 92-3, Department of Civil Engineering, The University of Texas at Austin, Austin, Texas*, 250 pp.
- Priestley, M.J.N., Seible, F. and Chai, Y.H. (1992). Design guidelines for assessment, retrofit, and repair of bridges for seismic performance. *Report No. SSRP-92/01, University of California at San Diego, San Diego, California.*
- Ricles, J., Priestley, M.J.N., Seible, F., Yang, R., Imbsen, R. and Liu, D. (1991). The Whittier Narrows 1987 earthquake: performance, analysis, repair and retrofit of the I-5/I-605 separator. *Report No. SSRP-91/08, University of California, San Diego, La Jolla, California.* 351 pp.
- Takeda, T. and Sozen, M.A. (1970). Reinforced concrete response to simulated earthquakes. *Journal of the Structural Division, ASCE, Volume 96, No. ST12*, pp. 2557-2573.

## ACKNOWLEDGMENT

The support provided by the Graduate School of the University of Wisconsin-Madison is greatly appreciated.